Chemotaxis of bacteria in glass capillary arrays

Escherichia coli, motility, microchannel plate, and light scattering

Howard C. Berg and Linda Turner

The Rowland Institute for Science, Cambridge, Massachusetts 02142; and Department of Cellular and Developmental Biology, Harvard University, Cambridge, Massachusetts 02138 USA

ABSTRACT Random and directed motility of bacterial populations were assayed by monitoring the flux of bacteria through a microchannel plate (a porous glass plate comprising a fused array of capillary tubes) separating two identical stirred chambers. Cells, washed free of growth medium by a new filtration method, were added to one chamber at a low density. Their number in the other chamber was determined from the amount of light scattered from a beam of a laser diode and recorded on a strip chart. Diffusion coefficients were computed from fluxes observed in the absence of chemical gradients, and chemotaxis drift velocities were computed from fluxes observed in their presence. Cells migrated through tubes of diam 10 μm more rapidly than through tubes of diam 50 μm, suggesting that the straight segments of their tracks were aligned with the axes of the smaller tubes. Mutants that are motile but nonchemotactic could be selected because they move through the microchannel plate in the face of an adverse gradient. Weak chemotactic responses were assessed from ratios of fluxes observed in paired experiments in which the sign of the gradient of attractant was reversed. Studies were made of wild-type *Escherichia coli* and mutants that are nonmotile, tumbly, smooth-swimming, aspartate-blind, or defective in methylation and demethylation. Chemotaxis drift velocities for the latter mutants (*cheRcheB*) were quite small.

INTRODUCTION

The track of a peritrichously flagellated bacterium appears as a series of approximately straight segments of random length, separated by turns of nearly random angle (Berg and Brown, 1972). The straight segments are generated by intervals, called runs, during which the cell swims steadily forward. The turns are generated by intervals, called tumbles, during which the cell moves erratically. When a cell swims in a chemical gradient, runs that happen to carry it in a favorable direction are extended. Thus, it drifts up gradients of attractants or down gradients of repellents.

In *Escherichia coli* (*E. coli*), both run and tumble intervals are exponentially distributed, with means of ~1 and 0.1 s, respectively, and the turn-angle distribution is biased somewhat in the forward direction (Berg and Brown, 1972). When grown on a rich medium and studied at 32°C, the cells swim 30–40 μm/s (Lowe et al., 1987). A single cell is ~1 μm in diameter by 2 μm long. For recent reviews of bacterial motility and chemotaxis, see Macnab (1987*a*, *b*), Stewart and Dahlquist (1987), Macnab and DeRosier (1988), Berg (1988), Bourret et al. (1989), Lengeler and Vogler (1989), and Stock et al. (1990).

To define the motile behavior of a population of cells (comprising a set of genetically identical individuals), one needs to measure both a diffusion coefficient, characterizing the random motility (the mean-square distance that cells wander in a given period of time; cf. Berg, 1983, Ch. 1) and a drift velocity, characterizing the chemotactic response (the mean distance that cells move up or down a specified gradient in a given period of time; cf. Berg, 1983, Ch. 4). If this is done with gradients that are relatively steep, weak responses can be quantified.

A method for doing this is described here, in which cells in motility medium migrate between two stirred chambers through a plate penetrated by a large number of small holes (through a glass capillary array of the sort used in microchannel-plate image intensifiers). Cells added initially to chamber 1 migrate to chamber 2, where their number is measured by the amount of light that they scatter from the beam of a laser diode. We compute diffusion coefficients from the flux of bacteria observed in the absence of chemical gradients. The flux increases when an attractant is added to chamber 2 or a repellent is added to chamber 1, and it decreases when an attractant is added to chamber 1 or a repellent is added to chamber 2. These changes allow us to compute chemotaxis drift velocities. We begin by measuring diffusion coefficients of wild-type cells and of a variety of nonchemotactic mutants that exhibit different tumble frequencies. Then we measure drift velocities of wild-type cells in gradients of different attractants or repellents. Next, we show that our apparatus can be used to select for mutants that are motile but unable to respond to specific attractants or repellents. Finally, we characterize a *cheRcheB* mutant (a cell defective in both methylation and demethylation) thought to be chemotactic by some workers (e.g., Stock et al., 1985) but not by others (e.g., Segall et al., 1986).

Our assay is reminiscent of that of Armitage et al.

0006-3495/90/10/919/12 $2.00

(1977), who count the number of bacteria that cross thin membranes separating two unstirred chambers in the course of 1 h. The main differences are that in our assay the microchannel plates are thick rather than thin, the gradients remain steep and nearly constant for the duration of the experiment, and the cell counts are made continuously, on-line.

Three other methods for studying chemotactic responses of bacterial populations should be mentioned: the swarm-plate assay (Adler, 1966; Armstrong et al., 1967), the capillary assay (Adler, 1969, 1973), and the layered-gradient assay (Dahlquist et al., 1972, 1976). In the swarm-plate assay, bacteria are inoculated near the center of a petri plate containing growth medium in semi-solid agar. As the cells take up nutrients, grow, and divide, they generate spatial gradients of chemical attractants. The cells chase these attractants, swarming outwards in concentric bands that scatter enough light to be visible to the naked eye. This assay is easy to carry out, but the response depends in a complicated way on transport, metabolism, and growth, as well as on motility and chemotaxis (Adler, 1966; Nossal, 1972; Wolfe and Berg, 1989).

In the capillary assay, bacteria are suspended in a medium that does not support growth. A capillary tube containing a solution of an attractant is inserted into this suspension. A spatial gradient is formed by diffusion of attractant from the tip of the capillary tube. The bacteria migrate up this gradient, and some enter the tube. They are counted later by serial dilution and plating. The capillary assay is subject to substantial variation, probably due to convection near the tip of the capillary tube during the time required for the gradients to form and the cells to respond. The number of bacteria that enter a tube not containing attractants provides a measure of the diffusion coefficient (Segel et al., 1977).

In the layered-gradient assay, a cuvette is filled with a uniform suspension of cells in the presence of two vertical gradients, one a density gradient that stabilizes the system against convection and the other a concentration gradient that provides a chemotactic stimulus. If the latter gradient is exponential, spanning a range of concentrations near the dissociation constant of the chemoreceptor and capped by a fixed plateau, the cells migrate up this gradient at a uniform speed and accumulate at the plateau. The distribution of cells is determined from the amount of light scattered at different points from a laser beam aligned with the gradient. This assay has the advantage that drift velocities can be determined accurately in gradients that are shallow but otherwise optimally defined. An estimate also can be made of the diffusion coefficient (Nossal and Weiss, 1973; Segel and Jackson, 1973).

MATERIALS AND METHODS

Chemicals[1]

Synthetic sodium L-aspartate and L-leucine were from ICN Biochemicals Inc. (Cleveland, OH), α-methyl-D, L-aspartate from Sigma Chemical Co. (St. Louis, MO), synthetic L-serine from K&K Laboratories Inc. (Cleveland, OH), and nickel(ous) chloride from Fisher Scientific Co. (Pittsburgh, PA). Isopropyl β-D-thiogalactoside (IPTG), polyvinylpyrrolidone (PVP-40), streptomycin sulfate, tetracycline hydrochloride, and thymine were from Sigma Chemical Co., sodium dodecyl sulfate (SDS, specially pure) from BDH Chemicals Ltd. (Poole, England), and tryptone, yeast extract, and agar from Difco Laboratories, Inc. (Detroit, MI). Other chemicals were reagent grade. Water was deionized (18 MΩ-cm) and filtered (0.2 μm).

Media

Motility medium was 0.067 M NaCl, 0.01 M potassium phosphate (pH 7.0), 0.01 M sodium lactate, 10^{-4} M EDTA, 10^{-6} M L-methionine, and 0.1% PVP-40 (added to minimize adsorption of bacteria to the glass capillary array; see below). Soap solution was 0.2% SDS, 0.02 M Tris-HCl (pH 7.0), 0.05 M EDTA (dipotassium salt). L broth was 1% tryptone, 0.5% yeast extract, 0.5% NaCl, 2×10^{-5} M NaOH. Tryptone broth was 1% tryptone, 0.5% sodium chloride.

Culture conditions

All strains were derivatives of *E. coli* K12 and are listed in Table 1. Crystals from frozen reference stocks were added directly to tryptone broth and grown to saturation at 34°C (30° for strains carrying phage), dimethyl sulfoxide was added (10% vol/vol), and 100μl aliquots were frozen at −75°C. These aliquots were thawed as needed, added to 10 ml

TABLE 1 Bacterial strains and phage*

Strain	Relevant genotype	Source or reference
AW405	wild type	Armstrong et al. (1967)
HCB5	*fliC*	P1(YK4106) × AW405‡
HCB437	Δ(*tsr*)7021 Δ(*trg*)100 Δ(*cheA-cheZ*)2209	Wolfe et al. (1987)
HCB626	RP5232 (λDFB19)	D. F. Blair
HCB627	HCB437 (λDFB19)	Wolfe et al. (1988)
HCB869	Δ(*tar-tap*)5201 *zac*::Tn*10*	P1(YYC85) × RP5854§
RP1273	Δ(*tap-cheB*)2241	Sherris and Parkinson (1981)
RP3087	*motB*580	cf. Block and Berg (1984)
RP5232	Δ(*cheY*)m60-21	J. S. Parkinson
RP5854	Δ(*tar-tap*)5201	J. S. Parkinson
λDFB19	p*lac-cheY*	cf. Wolfe et al. (1988)

*All strains are resistant to streptomycin. Tn*10* strains are resistant to tetracycline.
‡YK4106 is a *fliC* (formerly *hag*) strain obtained from M. I. Simon.
§YYC85 is a *zac*::Tn*10* strain isolated by Chang and Cronan (1982).

[1] *Abbreviations used in this paper:* IPTG, isopropyl β-D-thiogalactoside; PVP-40, polyvinylpyrrolidone of molecular weight 40,000; SDS, sodium dodecyl sulfate.

of tryptone broth (with or without IPTG), and grown to mid-exponential phase at 34°C (or 30°). This gave cultures whose motility was highly reproducible. Optical densities were measured at 610 nm with a UV-Visible spectrophotometer (model 139; Hitachi Perkin-Elmer, Danbury, CT). Conversion to cell densities was made with a factor (6.2×10^8 cells/ml per o.d. unit) determined by plating wild-type cells on T broth + 1.5% agar. All of the cultures grown for the present work had cells of approximately the same size (as judged by eye from videotapes made by phase-contrast microscopy), so the same factor was used for each. Wild-type cells were distinguished from tetracycline-resistant mutants by replica plating on L broth + 1.5% agar containing 2.5×10^{-5} M $MgCl_2$, 40 μg/ml thymine, and 125 μg/ml streptomycin sulfate, with or without 25 μg/ml tetracycline hydrochloride.

Preparation of cells

The washing technique used by Adler (1973) requires centrifugation and gentle resuspension. This proved too time consuming, so a new method was developed that allowed us to transfer cells from tryptone broth to a chemically defined medium in <10 min. Cells never clumped, and no loss in motility was apparent, as judged by eye by phase-contrast microscopy. A 1-l filter flask was equipped with the ground-glass base and stopper designed for 47-mm diam membrane filters (xx1004702; Millipore Corp., Bedford, MA). A type HATF filter (low water-extractable, 0.45-μm pore size), that had been soaked overnight in motility medium, was placed on top of the base and covered with a funnel machined from delrin (5.7 cm o.d. by 2.5 cm high). The base of the funnel was flat and formed an adequate seal with the filter without the use of any clamps. The hole at the center of the base was 1.2 cm in diameter. The inner wall of the funnel (3.6 cm i.d.) was vertical for about two-thirds of its height and then tapered to the hole at the bottom. The filter flask was equipped with a vacuum hose (connected to a rough vacuum) that had been cut in two a few centimeters from the flask. Suction, initiated by the abutment of the cut ends, was abruptly terminated when the ends were pulled apart. This made it possible to draw fluid through the filter without ever letting it run dry, i.e., to leave ~0.3 ml of fluid at the base of the funnel at the end of each filtration cycle. Proceeding in this fashion, 5 ml of culture was pipetted into the funnel and drawn through, followed by four successive 10-ml aliquots of motility medium. Then the funnel was lifted off, and the filter was rolled up with a pair of tweezers and placed in the mouth of an 18-mm diam culture tube. The tube was held vertically, and 7.5 ml of motility medium was used to rinse the cells from the filter into the tube. This gave a suspension with an optical density slightly greater than half of that of the original culture. When a series of experiments were to be run on the same sample, this suspension was stored at 4°C.

Motility apparatus

Two stirred chambers were separated by a microchannel plate (a porous glass plate comprising a fused array of capillary tubes), as shown in Fig. 1. Cells added to chamber 1 migrated through the microchannel plate and were detected by light scattered from a laser beam passing through chamber 2. The optical system was designed to take advantage of the fact that the most intense scattering is expected in the forward direction (cf. Born and Wolf, 1980). The laser was gated on and off to allow for phase-sensitive detection, as shown in Fig. 2. The chambers were identical, so that the contents of either one could be monitored and so that stirring in one chamber was the mirror image of that in the other. This minimized pressure gradients that might drive fluid through the microchannel plate via Poiseuille flow. For the same reason, connections to the input and output tubes at either chamber (made with 0.058 cm i.d. polyethylene tubing) were valved off when fluid was drawn through the other chamber (see below). The chamber assembly (3.9 cm long, 2.7 cm wide, 4 cm high) was placed in an insulated aluminum box that also supported the light source and the detector. Either chamber could be monitored by rotating the assembly 180°. The temperature of the box was sensed by a thermistor and controlled by a Peltier element (cf. Khan and Berg, 1983). The experiments were done at 30°C. Properties of the glass capillary arrays are summarized in Table 2.

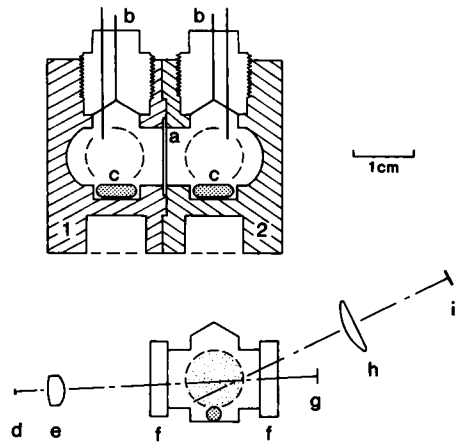

FIGURE 1 Scale drawings of the apparatus. (*Top*) Side view of chambers 1 and 2. (*Bottom*) Schematic of a section through the center of chamber 2 viewed from the right, including optics. The chambers, each of volume 1.8 cm^3, were machined from delrin, and separated by a microchannel plate (open diam 0.95 cm, thickness 0.05 cm) seen edge-on in the side view (*top*, *a*) and face-on in the end view (*bottom*, behind the plane of the section, shown speckled). The chambers were completely filled with motility medium. Additional medium containing cells, attractants, or repellents were drawn into either chamber through the tubes indicated at *b*. The contents of the chambers were stirred by counter-rotating stir bars (*c*). The optical-train included a diode laser (*d*), a collimating lens (*e*), a pair of silica windows (*f*), a beam stop (*g*), a collecting lens (*h*), and a photodiode (*i*). The components were (*a*) Galileo Electro-Optics Corp. (Sturbridge, MA) C13S05M10 or C13S05M50, made from soda lime glass, sandwiched between two silicon-rubber gaskets (Millipore SX00 013 01); (*b*) 22-gauge stainless-steel tubes in threaded delrin plugs (sealed with silicon-rubber gaskets) with entry to either chamber through the longer tube and exit through the shorter tube; (*c*) 7 × 2 mm teflon-coated stir bars driven 2 revolutions per s by counter-rotating external magnets (not shown); (*d*) Mitsubishi (Electric Corp., Tokyo, Japan) ML4402A, 780 nm, 3 mW; (*e*) Newport Corp. (Fountain Valley, CA) F-L40; (*f*) Melles Griot (Irvine, CA) 02WLQ103 cemented on face with silicone-rubber cement (GE RTV 118) and at the edges with a histological resin (Permount, Fisher Scientific Co.); (*g*) flat-black paint; (*h*) chosen empirically from a lens assortment to focus a 1-cm tungsten filament, used as a mock-up of the laser beam, onto a spot the size of the active area of the photodiode; (*i*) United Detector Technology (Hawthorne, CA) PIN-5DP, 0.25 cm active diameter.

Assembly of the apparatus

The glass capillary arrays (plates 13 mm in diameter by 0.5 mm thick) were stored in soap solution under rough vacuum. This prevented them

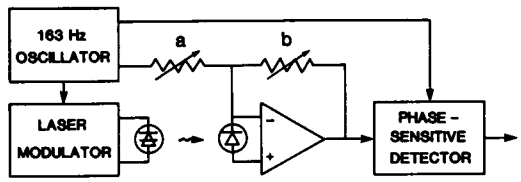

FIGURE 2 A block diagram of the cell detection system. A laser diode was switched on and off at 163 Hz by a circuit that also regulated its output (utilizing a photodiode that is part of the laser-diode assembly). Light scattered from the bacteria was detected by a silicon photodiode operating in the photovoltaic mode. The current-to-voltage converter has controls that (*a*) inject current, derived from a low-pass filtered square wave, to offset the signal due to light scattered from the chamber windows, and (*b*) adjust the gain. The output of this stage was fed to a phase-sensitive detector (4110; Evans Electronics, Berkeley, CA) with a 10-s low-pass filter time constant. The final output was connected to a strip-chart recorder (not shown). The input to the phase-sensitive detector and the input to the synchronous converter in that detector were monitored on an oscilloscope (not shown). Components not identified in Fig. 1: oscillator, ICM 7555; modulator, LF356 driving VN01; converter, LF356 with gain 1.3×10^7 V per amp.

from becoming clogged by bacteria and ensured that they were completely filled with fluid. Before assembly, an array was removed, rinsed with fresh soap solution (in a recess at the bottom of a funnel similar to that used for washing cells, but modified so that the array could not come into contact with the ground-glass base), then with water, and finally with motility medium. Then it was immersed in motility medium and returned briefly to rough vacuum. This was done to ensure that all of the capillary tubes were completely filled with liquid. The other parts of the apparatus, which also had been stored in soap solution, were rinsed with water and dried. Then the apparatus was assembled and filled from one side with motility medium that had been stored at 34°C. Because this medium cooled rather than warmed on approaching the operating temperature (30°C), the formation of air bubbles was suppressed. The threaded plugs containing the input and output tubes were screwed down, the polyethylene tubing was connected and purged of air, the stirrers were turned on, and the apparatus was allowed to stand for 20 min or more, until the light-scattering signal reached a stable baseline. Aliquots of cells or chemicals were added to either chamber by placing a measured drop of fluid on a sheet of parafilm, inserting the tip of the input line into the drop, opening the requisite valves, and applying gentle suction to the output line through a needle valve (cf. Berg and Block, 1984, Fig. 4). When the drop was exhausted, the input line was rinsed with an aliquot of motility medium. A single-pole double throw valve (type HVP 86778; Hamilton, Reno, NV) was used to connect the needle valve to either chamber, and a double-pole double-throw valve (#86779) was used at either chamber to connect the input tube to the output tube (isolating the chamber) or to connect the input line to the input tube and the output line to the output tube (allowing exchange of media).

TABLE 2 Properties of glass capillary arrays (microchannel plates)

Pore size*	Tube length	Fraction of area open‡	Number of exposed tubes§	Area of tube walls‖	Mean no. bacteria/tube¶
μm	μm			cm^2	
10	500	0.67	6.1×10^5	96	0.2
50	500	0.52	1.9×10^4	15	4.9

*Nominal diameter of capillary tubes.
‡Areas measured from photomicrographs with a planimeter (model N-10; Los Angeles Scientific Instruments Co., Los Angeles, CA). The 10-μm pores are approximately hexagonal in cross-section (10.0 μm side-to-side, 11.2 μm vertex-to-vertex), the 50-μm pores more nearly circular. Both are closely packed.
§Not covered by the gaskets. Plate outside diam 1.30 cm, gasket inside diam 0.95 cm, gasket inside area 0.71 cm^2.
‖Total for exposed tubes, assuming circular cross-sections.
¶Assuming 10^7 bacteria/ml in chamber 1 and 0 in chamber 2, i.e., 0.5×10^7 bacteria/ml in the tubes.

THEORY

Preliminary estimates

We will assume that the concentrations of cells and chemicals are uniform in both chambers, i.e., that the stirring is efficient. We expect wild-type *E. coli*, when moving randomly, to have a diffusion coefficient, D, of order 4×10^{-6} cm^2/s (Berg, 1983, p. 93, assuming a run velocity of $\sim 3 \times 10^{-3}$ cm/s and a run interval of 1 s) and, when exposed to a steep gradient of a good attractant, to have a drift velocity, v, of order 4×10^{-4} cm/s (Dahlquist et al., 1972). The time required for a cell to traverse a capillary tube of length d by random motility is of order $d^2/2D$ (Berg, 1983, p. 10), whereas the time required for it to do so by drift is d/v. Therefore, if we are to distinguish the two, we must have $d/v < d^2/2D$, or $d > 2D/v \approx 0.02$ cm. The capillary arrays that we have used (Fig. 1) are stocked in thicknesses ranging from 0.05 to 0.20 cm. For most of our work, we chose $d = 0.05$ cm to minimize the time required for the diffusive flux to approach its steady-state value, which is $\sim d^2/2D \approx 5$ min. The same formula, $d^2/2D$, governs the time required for a chemical gradient to be established after the addition of an attractant or a repellent, where now the migration is driven by thermal energy. For aspartate or serine, $D \approx 10^{-5}$ cm^2/s, so this time is of order 2 min. Cells that are not motile have diffusion coefficients of order 10^{-9} cm^2/s (Berg, 1983, p. 93) and are not expected to move through the microchannel plate in a reasonable time ($d^2/2D \approx 2$ wk).

Steady-state behavior

Most of our data were collected after steady-state conditions had been established but before the initial concentrations of cells in chamber 1 or of chemicals in chamber 1 or chamber 2 had time to change by more than a few percent. During this period, the steady-state flux of cells, J (in cells per square centimeter per second), can be computed from the equation for one-dimensional

diffusion with drift (Berg, 1983, p. 51):

$$J = -D(\partial C/\partial x) + vC, \quad (1)$$

where the concentration of cells, C, is equal to the initial concentration, C_0, at $x = 0$ and to 0 at $x = d$. The total number of cells entering chamber 2 per second is JA, where A is the total cross-sectional area of the capillary tubes, and the time-rate of change in density of cells in chamber 2 is JA/V, where V is the volume of chamber 2. The slope of the strip-chart record provides a direct measure of JA/V.

As a first approximation, we assume that the drift velocity, v, is constant. Eq. 1 then takes the form $\partial C/\partial x = (vC/D) - (J/D)$, where J is a constant that remains to be determined. Integration of this equation and application of the boundary conditions at $x = 0$ and $x = d$ gives $C = C_0[\exp(d/l) - \exp(x/l)]/[\exp(d/l) - 1]$ and $J = C_0 v \exp(d/l)/[\exp(d/l) - 1]$, where l is the characteristic length D/v. In the limit $v \to 0$, one can show that $C \to C_0(d - x)/d$ and $J \to C_0 D/d$, as expected for diffusion without drift (Berg, 1983, p. 19).

Fig. 3 shows values for C/C_0 for $d = 0.05$ cm and $l = D/v = -0.01$ cm (negative drift), $v = 0$ (zero drift), and $l = 0.01$ cm (positive drift). Because $C \to 0$ as $x \to d$, the second term in Eq. 1 vanishes there, i.e., the value J is proportional to the steepness of the cell gradient at $x = d$. Note that the values of J differ markedly from one another only when the length $l = D/v$ is smaller in amplitude than d, i.e., only when the amplitude of the exponent $d/l = dv/D$ is large. Thus, to distinguish fluxes due to chemotaxis from those due to diffusion, we require a plate of thickness $d > D/v$.

The ratios of the fluxes observed with and without drift provide a sensitive means of gauging the amplitude of a chemotactic response. For positive drift, v (and hence l) are positive, and $J_+ = C_0 v \exp(d/l)/[\exp(d/l) - 1]$.

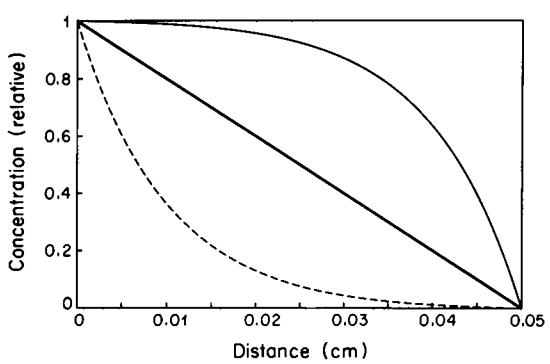

FIGURE 3 Concentrations of bacteria expected in capillary tubes 0.05-cm long as a function of the distance from chamber 1, assuming that with attractants or repellents $D/v = \pm 0.01$ cm. (*Top*) positive drift; (*middle*) zero drift; (*bottom*) negative drift.

For negative drift, v (and hence l) are negative. Treating v and l hereafter as amplitudes (i.e., as positive quantities), $J_- = -C_0 v \exp(-d/l)/[\exp(-d/l) - 1] = C_0 v/[\exp(d/l) - 1]$. As noted above, $J_0 = C_0 D/d$. Therefore

$$J_+/J_0 = (d/l)\exp(d/l)/[\exp(d/l) - 1], \quad (2)$$

$$J_-/J_0 = (d/l)/[\exp(d/l) - 1], \quad (3)$$

and

$$J_+/J_- = \exp(d/l). \quad (4)$$

For $d/l = dv/D = 5$, these ratios are ~5, 1/30, and 150, respectively. That is, if we do an experiment in which we add cells to chamber 1, measure the flux J_0, and then add a strong attractant to chamber 2, the flux should increase by a factor of ~5. If we do an experiment in which we add cells to chamber 1, measure the flux, and then add a strong attractant to chamber 1, the flux should decrease by a factor of ~30. If the chemotactic response is weak, so that dv/D is small, or if the attractants or repellents perturb D by changing swimming speeds or run intervals, an estimate of the magnitude of v can still be made by reversing the gradient and measuring $J_+/J_- = \exp(dv/D)$.

This analysis predicts that the ratio of fluxes observed when one changes the sign of the chemical gradient should increase exponentially with the plate thickness, d. However, we do not expect this to occur in practice, because the chemical gradients are linear, not exponential. We know that the chemotactic response is proportional to the time rate of change in the fraction of receptor bound (cf. Block et al., 1983). In a linear gradient, this change is large only when the concentration is small. As a result, the drift velocity, v, is not constant. Thus, adding to the length of the capillary tube and to the initial concentration of the chemical (to maintain a constant gradient) should not change the ratios J_+/J_0 or J_-/J_0 by a large factor. A computer simulation of the approach to steady state that included the proper dependence of v on the concentration of an attractant verified this expectation (data not shown).

Variable diffusion coefficient

J_+/J_- should be insensitive to variations in flux due to local changes in diffusion coefficient, provided that those changes are due to changes in tumble frequency rather than speed (cf. Schnitzer et al., 1990). For example, if a substance that suppresses tumbles is added to chamber 2, so that D varies across the microchannel plate as $D = D_0(1 + \alpha x)$, where α is constant, and that substance is not a chemoattractant, so that $v = 0$, then Eq. 1 has the solution $C = C_0 - (J/\alpha D_0)\ln(1 + \alpha x)$. As before, we

have assumed that $C = C_0$ at $x = 0$, $C = 0$ at $x = d$, and J is constant. If the same substance is placed in chamber 1, instead, so that $D = D_0(1 - \alpha x + \alpha d)$, then Eq. 1 has the solution $C = C_0 - (J/\alpha D_0) \ln [(1 + \alpha d)/(1 - \alpha x + \alpha d)]$. In either case, $J = C_0 \alpha D_0 / \ln (1 + \alpha d)$.

Departure from steady-state behavior

When measuring chemotactic drift rates, it is not necessary to worry about the cells in chamber 2 that return to chamber 1: when the drift velocity is negative, too few cells reach chamber 2 to matter; when the drift velocity is positive, the cells that reach chamber 2 are not able to get back. A problem arises only when one measures diffusive fluxes over long periods of time. After long times, instead of $J_0 = C_0 D/d$, one has $J_0 = (C_1 - C_2)D/d$, where C_1 and C_2 are the concentrations of cells in chambers 1 and 2, respectively. Because the total number of cells is constant and the volumes of the two chambers are the same, $C_1 + C_2 = C_0$, and one can show that C_1 decays exponentially to $C_0/2$ with a time constant $dV/2AD$, which for our experiments is equal to a few hours. In any event, because C_0 is known and the strip-chart record indicates C_2, one can easily compute C_1.

RESULTS

Raw data

Strip-chart records for two experiments are shown in Fig. 4. The full-scale sensitivity (1.0 on the ordinate) was 7×10^5 cells/ml. Note that the noise level was more than a factor of 100 smaller than this; therefore, we could reliably measure the light scattered from a few thousand cells/ml. This made it possible to work with cells at an initial concentration of 10^7/ml or less, where oxygen levels remained adequate for vigorous motility for many hours. Noise levels were generally better after the components of the chambers had soaked for a day or more in soap solution. For example, they were noticeably higher in the second experiment shown in Fig. 1 than in the first: compare the fluctuations at *g* to those at *a*. When cells were drawn into chamber 1 at *a*, no change in the light-scattering signal was seen. This indicates that cells were not driven into chamber 2 by bulk flow. However, when aspartate was added to chamber 2 at *f*, the baseline shifted slightly. Evidently, some of the material in this sample scattered light. Shifts of this kind were generally smaller than that shown. The downward shift at *c* was expected, because the contents of chamber 2 were diluted by the addition of the aspartate by ~10%. The mixing time in either chamber was at most a few seconds,

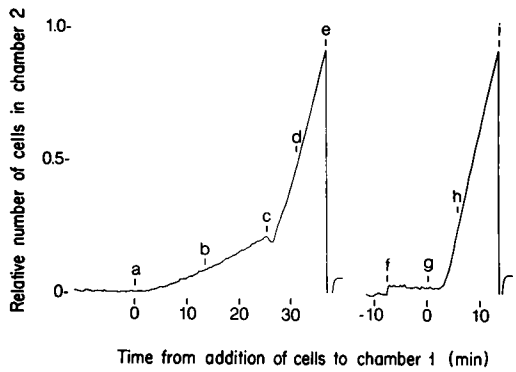

FIGURE 4 A photocopy of a strip-chart record showing diffusion of cells of wild-type strain AW405 and their responses to positive gradients of L-aspartate in a 10-μm capillary array. Cells were added at time 0; the full-scale sensitivity was 7×10^5 cells/ml. In the experiment shown on the left, cells were added first and the attractant second. In the experiment shown on the right, the additions were made in the opposite order. The record begins after the apparatus had been assembled and allowed to stand for ~40 min (*left*). At *a* cells were added to chamber 1 (0.26 ml with rinse, final concentration 5×10^6 cells/ml). The slope measured between *b* and *c* gave $D = 6.6 \times 10^{-6}$ cm^2/s. At *c* L-aspartate was added to chamber 2 (0.17 ml with rinse, final concentration 5 μM). The slope measured between *d* and *e* gave $v = 8.2$ μm/s. At *e* the laser was turned off, the apparatus was turned 180°, the detector was attenuated by a factor of 100, and the laser was turned on; this provided a measurement of the number of cells remaining in chamber 1. Then the apparatus was taken apart and cleaned, reassembled, and allowed to stand for ~40 min (*right*). At *f* L-aspartate was added to chamber 2. At *g* cells were added to chamber 1. The slope measured between *h* and *i* gave $v = 7.4$ μm/s. Finally, the number of cells remaining in chamber 1 was measured, as before.

substantially smaller than the decay time due to the detector low-pass filter, which was 18 s (data not shown). The time span from *a* to *b* was ~13 min: the time required to establish steady-state diffusion of cells across the capillary tubes (see below). The time span from *c* to *d* was ~6 min: the time required to establish a steady-state gradient of attractant across the capillary tubes and for cells (some already inside the tubes) to form the distribution expected for positive drift (Fig. 3). The time span from *g* to *h* was ~5 min: the time required for the cells to establish such a distribution in response to a pre-formed gradient of aspartate.

Simple diffusion

The behavior shown in Fig. 4 for random motility (*a–c*) was fairly typical. The time span from *a* to *b* tended to be relatively short for strains with large diffusion coefficients and relatively long for strains with small diffusion coefficients, as expected from the relationship $t \approx d^2/2D$. At later times, the slope was approximately linear, curving downwards only when a significant fraction of cells had

moved from chamber 1 to chamber 2. In our early work, measurements of the number of cells leaving chamber 1 did not agree with the number entering chamber 2, and when the same number of cells was added to both chambers, cells disappeared from both. This suggested that cells were being adsorbed on the walls of the capillary tubes, whose areas are large (Table 2, next to last column). This problem was solved by the addition of PVP-40 to the motility medium. Several neutral detergents also worked, but then the noise level increased, presumably due to light scattered by detergent micelles. For some cultures of a particular strain, the span *a–b* was prolonged: the trace continued to curve upwards for a much longer time. We believe that a substantial number of cells in these cultures swam poorly, skewing the distribution of diffusion coefficients to lower values. A distribution of diffusion coefficients computed from earlier tracking data (data for *E. coli* cited by Lowe et al., 1987) was found to be skewed in this direction (data not shown). Therefore, the curvature seen in Fig. 4 (between *a* and *b*) was probably due, in part, to variations in the motile behavior of different cells in the culture.

Diffusion coefficients measured with 10- and 50-μm diam capillary-tube arrays are compared in Table 3. For each culture, measurements of $D = dJ_0/C_0$ were made with one array, the apparatus was taken apart, cleaned, and reassembled, and the measurements were repeated with the other array. Sometimes this cycle was repeated.

Nonmotile cells provided a control for bulk flow that might be generated by pressure gradients due to stirring (Table 3, row 1). No such flow was detectable with the 10-μm array, whereas the 50-μm array gave an apparent diffusion coefficient of 7×10^{-8} cm^2/s. Because this value is ~30 times larger than the value expected for Brownian movement (see above), some bulk flow occurred with the 50-μm array. Now, for a given pressure drop, the rate of flow through a circular pipe (Poiseuille flow) is proportional to the fourth power of its diameter. But the number of pipes per unit area of a capillary array is inversely proportional to the square of the diameter. Therefore, we would expect bulk flow to increase with the square of the capillary-tube diameter. This implies that bulk flow through the smaller array should give an apparent diffusion coefficient of order 3×10^{-9} cm^2/s, approximately equal to the value expected for Brownian movement. We conclude that bulk flow is not a problem, particularly for experiments made with the 10-μm array. To rule out the possibility that motion of nonmotile cells was hindered in the small tubes by the inert flagella, the experiment with the 10-μm array was repeated with a strain lacking flagellar filaments (Table 3, row 2): no change in baseline was evident in 4 h.

A strain whose cells tumble incessantly or swim slowly with right-handed flagellar bundles (strain HCB626 induced with 200 μM IPTG; cf. Wolfe and Berg, 1989) gave diffusion coefficients that were relatively small with both the 10- and 50-μm arrays (Table 3, row 3).

Experiments with strain HCB627, in which the level of expression of *CheY* was progressively lowered and the cells swam progressively more smoothly, revealed surprising differences between the 10- and 50-μm arrays (Table 3, rows 4–7). With the 10-μm array, the diffusion coefficients increased monotonically, as expected. However, they were substantially larger than those measured with the 50-μm array. With the 50-μm array, the diffusion coefficients increased and then decreased, spanning a range of values that was relatively narrow.

With wild-type cells, the diffusion coefficient measured with the 10-μm array was more than twice as large as that measured with the 50-μm array (Table 3, last row). Measurements on cells from 10 wild-type cultures with the 10-μm array gave a mean and SD $(5.19 \pm 1.01) \times 10^{-6}$ cm^2/s, whereas measurements on cells from 4 wild-type cultures with the 50-μm array gave a mean and SD $(2.63 \pm 0.42) \times 10^{-6}$ cm^2/s. A similar difference was observed in measurements of drift velocities (see below).

We conclude that the motile behavior of the cells is modified by interactions with the capillary-tube walls. This does not appear to be due to adsorption (because cells were not lost; see above), or simply to a decrease in run lengths due to collisions with the walls (because diffusion coefficients were larger for smaller tubes), but rather to guidance. Evidently, in tubes of 10-μm diam, the cells move primarily in one dimension, up or down the pipe: they do not have room to swim crosswise. In tubes of 50-μm diam, smooth-swimming cells appear to be delayed at the walls (see Discussion).

TABLE 3 Diffusion of different cell types through 10- and 50-μm diameter capillary-tube arrays

Strain	IPTG*	Phenotype‡	D (10^{-6} cm^2/s)	
			10-μm array	50-μm array
	μM			
RP3087		nonmotile	<0.01	0.07
HCB5		nonmotile	<0.01	
HCB626	200	very tumbly	0.4	0.6
HCB627	40	tumbly	1.1	0.7
	20	less tumbly	1.9	1.0
	10	nearly smooth	6.5	1.3
	0	smooth	9.1	1.1
HCB437		smooth	7.2	1.1
AW405		wild-type	6.1	2.6

*Used to induce p*lac-cheY*; see Table 1.

‡As judged by eye from video tapes of cells from the same culture viewed by phase-contrast microscopy. Note: RP3087 has flagellar filaments that fail to turn; HCB5 lacks flagellar filaments.

Diffusion with positive drift

Positive responses of wild-type cells to the attractants L-aspartate and L-serine are shown in Fig. 5. Note that the drift velocities toward aspartate were larger with the 10-μm array than with the 50-μm array (by about the same factor as found for the diffusion coefficients, above). This was true for all of the concentrations tested. Measurements on cells from six cultures with the 10-μm array at 5-μM aspartate gave a mean ± SD 7.04 ± 1.12 μm/s, whereas measurements in cells from three cultures with the 50-μm array at the same concentration gave a mean ± SD 3.14 ± 0.91 μm/s. Drift velocities for serine and aspartate were roughly the same (Fig. 5). The responses declined somewhat at concentrations approaching 100 μM. This was expected because at these concentrations, the receptors approach saturation when the cells are at the top of the gradient (see Discussion). Drift velocities in gradients of 5–15- or of 10–20-μM aspartate were ~30% smaller than they were in gradients of 0–10-μM aspartate (data obtained with the 10-μm array, not shown).

Positive responses of wild-type cells to the repellents nickel and L-leucine also were measured. In these experiments, the repellent and the cells were both added to chamber 1. Only the 10-μm array was tested. The nickel response peaked at ~1.4 μm/s at a concentration of 40 μM and then declined, falling to zero at 1,000 μM, because the cells became nonmotile (data not shown). The leucine response continued to rise, reaching 3.7 μm/s at 10 mM, the highest concentration tested (data not shown).

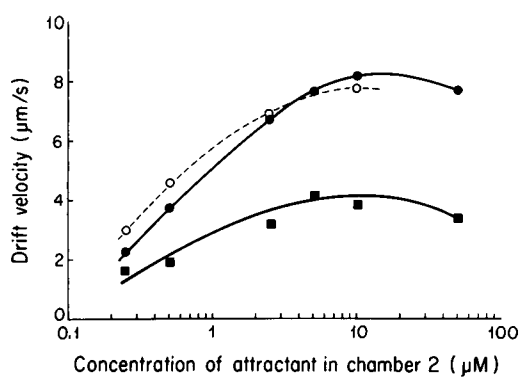

FIGURE 5 Drift velocities of cells of the wild-type strain (AW405) in positive gradients of attractants, computed from $v = J_+/C_0$. Note the semilog plot. The upper curves were obtained with the 10-μm array, the lower curve with the 50-μm array. Closed symbols and solid lines: L-aspartate. Open symbols and dashed line: L-serine. Usually, the 1st, 3rd, and 5th, points were obtained with one setup, the apparatus was taken apart and cleaned, and the 2nd, 4th, and 6th points were obtained with a second set-up. Attractant was added to chamber 2, cells were added to chamber 1, and then two further additions of attractant were made to chamber 2.

Diffusion with negative drift

A crude estimate of the flux expected when the sign of the gradient is reversed, e.g., when aspartate is added to chamber 1 rather than to chamber 2, can be made from the results obtained thus far. Assuming a drift velocity $v = (7.04 \pm 1.12) \times 10^{-4}$ cm/s and a diffusion coefficient $D = (5.19 \pm 1.01) \times 10^{-6}$ cm^2/s (see above), we compute a characteristic length $l = D/v = (7.37 \pm 1.70) \times 10^{-3}$ cm and a tube-length/characteristic-length ratio $d/l = dv/D = 6.78 \pm 1.57$. The standard deviation in this ratio, which we have estimated from the theory of propagation of errors (cf. Bevington, 1969) reflects a variation in behavior from culture to culture. Because v was determined experimentally from $J_+ \approx C_0 v$ and D was determined experimentally from $J_0 = C_0 D/d$, d/l is just J_+/J_0 (compare Eq. 2). The standard deviation is sufficiently large that all we can predict from Eq. 4 is that J_+/J_- should fall somewhere in the range of a few hundred to a few thousand.

Clearly, an accurate determination of J_+/J_- requires successive sets of measurements on cells from the same culture. In one, attractant is added to chamber 2 and allowed to form a gradient, and then cells (pre-adapted to 30°C) are added to chamber 1. This yields J_+ (as before). In the other, attractant is added to chamber 1 and allowed to form a gradient, and then cells (pre-adapted to 30°C and to the attractant) are added to chamber 1. This yields J_-. Data for three such experiments are summarized in Table 4, two for wild-type cells (strain AW405) and one, as a control, for cells of an aspartate-blind mutant (strain HCB869). For the wild type, the ratio J_+/J_- was several hundred, as predicted, and for the mutant, it was essentially 1. $J_+/J_- = 360$ implies (by Eq. 4) $d/l = dv/D = 5.89 \approx 6$, in agreement with the value estimated above from J_+/J_0. Thus, for wild-type cells and a linear aspartate gradient extending from 0 to 5 (or 10) μM, we have $J_+/J_0 \approx 6$, $J_-/J_0 \approx 1/60$, and $J_+/J_- \approx 360$. The value of J_0 expected for the wild type is 1,040 cells/cm^2 s, assuming $D = 5.2 \times 10^{-6}$ cm^2/s and $C_0 = 1 \times 10^7$ cells/cm^3. For the aspartate-blind mutant, we expect $J_+ = J_- = J_0$. Because the values for J_+ and J_- were

TABLE 4 Paired measurements of J_+ and J_- through a 10-μm array*

Strain	Phenotype	Asp concentration	Flux J_+	Flux J_-	J_+/J_-
		μM	*cells/cm^2 s*		
AW405	wild-type	5	6760	17	398
		10	6120	19	322
HCB869	asp-blind	100	415	469	0.88

*$C_0 = 1 \times 10^7$ cells/cm^3.

~440 (Table 4), this strain had a smaller diffusion coefficient than the wild type.

Selection of motile nonchemotactic mutants

The data in Table 4 suggest a method for selecting mutants that, while motile, fail to respond to one or more attractants. For example, if we were to add aspartate to chamber 1 and allow the gradient to form and then add equal numbers of cells of strains HCB869 and AW405 to chamber 1, we would expect mutant and wild-type cells to reach chamber 2 in the ratio 469:18 = 26:1 (Table 4, next to last column). To test this idea, we mixed cells of these two strains in the ratio 1:200 and exposed them to a negative gradient of α-methyl-D,L-aspartate (a nonmetabolizable analogue of aspartate, 300 μM in chamber 1), waited for ~20 min, and then sampled and plated the contents of chamber 2. Growth of contaminants was suppressed by addition of streptomycin, and cells of the aspartate-blind mutant were distinguished by their resistance to the antibiotic tetracycline. The ratio of mutant to wild-type cells was ~1:5, corresponding to enrichment of the mutant by a factor of ~40. Enrichments of ~40 also were found when the cells were mixed in the ratio 1:50 and harvested after ~60 min.

Characterization of mutants that are weakly chemotactic

Measurement of the J_+/J_- ratio provides a sensitive means of judging whether a particular strain is able to respond to an attractant or a repellent, particularly when the substance in question affects D (perturbs random motility; see the paragraph in Theory on variable diffusion coefficient). A case in point are double mutants defective in the methyltransferase (the product of the *cheR* gene) and the methylesterase (the product of the *cheB* gene), enzymes that are required for adaptation. Strain RP1273 (Table 1) is deleted for both *cheR* and *cheB*. When cells of this strain are tethered, the fraction of time that they spin counterclockwise can be shifted up or down at will by adding or subtracting aspartate (Segall et al., 1986). These changes occur in a fraction of a second. However, some cells appear to adapt, at least in part, over a relatively long time span (minutes). Also, nearly 10–100 times as much aspartate is required to produce a response in this strain as in the wild type. Thus, when cells of strain RP1273 move in a gradient, their random motility varies from place to place, and to some extent, from time to time. How does one decide whether or not these cells are chemotactic?

Probably the best that one can do is to compare fluxes in positive and negative gradients, gradients that are identical except for sign. Experiments of this kind are summarized in Table 5. Measurements were made in gradients of aspartate or serine, or in gradients of aspartate with a uniform background of serine (note [‖]) or in gradients of serine with a uniform background of aspartate (note [¶]). The first thing to note is that when aspartate was examined alone (cultures 1, 3, 4), the fluxes were relatively small. The diffusion coefficients measured for cells in 50, 100, or 1,000 μM aspartate (added to both chambers; data from four experiments, not shown) were roughly the same, $\sim 0.7 \times 10^{-6}$ cm^2/s, in approximate agreement with the value computed from the mean of the fluxes given in Table 5 at 100- and 1,000-μM aspartate, 0.89×10^{-6} cm^2/s. In the absense of aspartate or serine, the diffusion coefficient was even smaller, about one-third as large (data not shown). For aspartate alone, the mean value of J_+/J_- was 2.1, corresponding to a value of $d/l = dv/D = 0.74$ (Eq. 4), which if $D \approx 10^{-6}$ cm^2/s, gives $v \approx 1.5 \times 10^{-5}$ cm/s. This is only 2% of the value found with wild-type cells, even though the gradients are 10–100 times steeper. In a uniform background of serine (cultures

TABLE 5 Paired measurements of J_+ and J_- through a 10-μm array for strain RP1273*

Attractant	Concentration	Culture No.‡	Flux§ J_+	Flux§ J_-	J_+/J_-
	μM		cells/cm^2 s		
Aspartate	100	1	254 (1)	104 (2)	2.44
		3	194 (2)	83 (1)	2.34
	1,000	4	270 (1)	174 (2)	1.55
	100‖	8	689 (2)	1020 (1)	0.68
				685 (3)	1.01
		9	743 (1)	531 (2)	1.40
			502 (3)		1.06
Serine	100	2	199 (1)	95 (2)	2.09
		5	282 (1)	129 (2)	2.19
		10	158 (2)	614 (1)	0.26
				154 (3)	1.03
		11	315 (2)	1070 (1)	0.30
				137 (3)	2.30
		12	427 (1)	137 (2)	3.12
			154 (3)		1.12
	1,000	4	899 (1)	780 (2)	1.15
		6	968 (1)	612 (2)	1.58
		7	1020 (1)	802 (2)	1.27
	100¶	13	705 (1)	718 (2)	0.98
		14	830 (2)	780 (1)	1.06

*$C_0 = 1 \times 10^7$ cells/cm^3. For measurements of J_+, attractant was added to chamber 2; for measurements of J_-, it was added to chamber 1. In the latter case, the cells were pre-adapted to the attractant for 15 min.
‡Numbered in the order that the cultures were grown.
§The numbers in parenthesis indicate the order in which measurements on cells from a given culture were made.
‖With serine (100 μM) added to both chambers.
¶With aspartate (100 μM) added to both chambers.

8, 9) the fluxes were larger, but the response to the gradient vanished (mean value of J_+/J_- 1.04). Note that a ratio of 1.1 gives $v \approx 1.9 \times 10^{-6}$ cm/s, which is only ~0.3% of the drift velocity found with wild-type cells. But now, and in most of the other measurements involving serine (Table 5), the order in which the measurements were made mattered: fluxes that were measured first always were larger (except when cells were tested in a uniform background of aspartate, cultures 13, 14). This difference was traced to the period of time that the cells sat in motility medium before being exposed to serine. If this interval was short, the cells swam more smoothly. The reason for this is not understood. However, it might not have anything to do with the mutant phenotype: wild-type cells in motility medium also swim more smoothly when exposed to serine (cf. Berg and Brown, 1972, Fig. 5). In any event, the responses to serine, if real, did not appear to be very different from those to aspartate, and they vanished when the measurements were made in a uniform background of aspartate (cultures 13, 14). The weak responses seen in the absence of a uniform background of serine or aspartate might be an artifact resulting from suppression of the tumbly phenotype observed (both by measurement of J_0 and under the microscope) when cells of strain RP1273 are in motility medium. We conclude that *cheRcheB* cells are not chemotactic.

DISCUSSION

We have shown that it is possible to use light scattering to accurately measure the flux of bacteria that swim through a microchannel plate separating two stirred chambers. The holes through this plate are packed closely enough together that the flux is relatively large (in the absence of chemical gradients, $\sim 10^3$ cells/cm^2 s for $C_1 = 10^7$ wild-type cells/cm^3). The channels are thin enough to suppress bulk flow due to pressure gradients generated by stirring. Finally, the channels are long enough to distinguish random motility from diffusion with drift that characterizes chemotaxis. For wild-type cells in tubes 10 μm in diameter by 0.05 cm long, the flux observed in a positive gradient of 0–10 μM aspartate is 6 times larger than that observed in its absence, and the flux observed in a negative gradient of 10–0 μM aspartate is 60 times smaller than that observed in its absence. These factors are those expected for a chemotaxis drift velocity $v \approx 7$ μm/s, which is about one-fifth of the swimming speed measured by three-dimensional tracking (Lowe et al., 1987). The flux observed in the absence of a gradient implies a diffusion coefficient $D \approx 5 \times 10^{-6}$ cm^2/s (neglecting unstirred layers; see below).

The values of D and v for the tubes of diam 10 μm are substantially larger than those for the tubes of diam 50 μm (Table 3; Fig. 5). As noted earlier, this suggests that the motion in the smaller tubes is predominantly one-dimensional. Cells in these tubes do not have room to swim crosswise: the geometrical constraints are illustrated in Fig. 6. Evidently, after a cell in the smaller tube tumbles, it swims up or down the tube, rather than choosing a new direction at random. Clearly, the cell is able to make such a choice because the values of D tend to increase with run length (Table 3), and the values of v depend on the steepness of the gradient in a regular way (Fig. 5). Presumably, this would not be possible in a very small tube, because the cell would not have room to reorient its flagellar bundle or turn around.

A separate question is why diffusion coefficients measured in tubes of diam 50 μm fail to increase monotonically with run length (Table 3, rows 6 and 7). Also, why are the values for smooth-swimming cells smaller than those for wild-type cells (rows 7–9)? These results suggest that smooth-swimming cells spend a substantial fraction of their time trapped on the tube walls. A likely possibility is that they swim along the surface in circles. One often sees smooth-swimming cells do this under the microscope, moving clockwise on the surface of the slide and counterclockwise at the coverslip. A track of one such cell is shown in Fig. 7. These directions of rotation are expected, given that the flagellar bundle spins counterclockwise (when viewed from the tip toward the cell body) and the cell body rolls clockwise (cf. Macnab, 1987*a*). We built scale models of a brass bacterium in large and small lucite tubes, as shown in Fig. 6, to convince ourselves that such circular motion is possible at the surface of a tube of diam 50 μm. In the smaller tube, this maneuver tends to align the cell with the tube axis.

The diffusion coefficient expected for a cell swimming at a constant speed s in one dimension with runs exponentially distributed with mean duration τ is $D = s^2\tau$ (Berg, 1983, p. 93). For $s \approx 3.5 \times 10^{-3}$ cm/s and $\tau \approx 1$ s, $D \approx 1.2 \times 10^{-5}$ cm^2/s. Note that a run length of $s\tau = 35$ μm is substantially shorter than the length of the tube (500

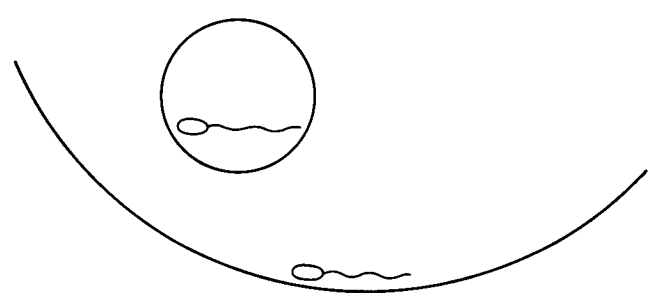

FIGURE 6 Scale drawings of a cell cross-wise in a tube of diam 10 μm or cross-wise near the wall of a tube of diam 50 μm. In the smaller tube, the cell does not have room to swim crosswise.

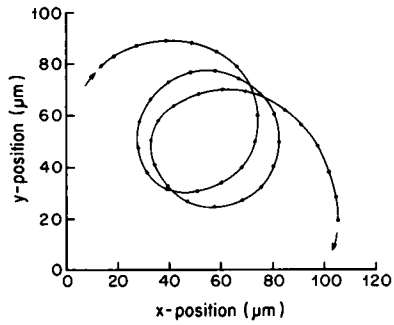

FIGURE 7 The path of a cell of the smooth-swimming strain *cheC497* (Armstrong and Adler, 1969) moving along the bottom window of the tracking chamber. During the period shown, the cell completed two loops ~48-μm in diameter. The tracking began at the upper left and continued for 21 s (time span between points 0.48 s). The *z*-position (not shown) remained constant to within ~±3 μm. The swimming speed averaged 21 μm/s. These data were collected in 1971 with the tracking microscope (Berg, 1971, 1978). For other data on this cell type, see Berg and Brown (1972).

μm), so that it is meaningful to describe one-dimensional migration of the cells in terms of diffusion with drift (Eq. 1). Why did we not observe values of D as large as 1.2×10^{-5} cm^2/s? One possibility is that cells do not swim as fast in the tubes as they do in free suspension. Another possibility is that they tumble more frequently there. A third possibility is that the effective thickness of the plate is >0.05 cm, because the medium immediately adjacent to it is not well stirred. By ignoring unstirred layers and computing D from dJ_0/C_0, we underestimated D. Note that this ambiguity does not affect measurements of v, because in the equations that relate v to J_+ or J_-, D always appears in the ratio $D/d = J_0/C_0$.

As noted earlier, the values of the drift velocity are expected to be larger at the bottom of the gradient than at the top: the gradients are linear, and the logarithmic derivative $(dC/dx)/C$ is large where C is small; cf. Block et al. (1983). Therefore, the values of v that we have measured represent an average over the length of the tube. Or to put it more precisely, the steady state distributions of cell concentrations for positive or negative drift are not quite the same as those shown in Fig. 3. As expected (Fig. 5), v is maximum when the concentration at the top of the gradient is only a few times larger than the dissociation constant of the receptor (~5 μM for aspartate or serine; cf. Clarke and Koshland, 1979). If allowance is made for differences between one- and three-dimensional swimming, the values for the drift velocities that we have observed are in the same range as those found with the layered-gradient assay (Dahlquist et al., 1972).

Given the relatively large depression in flux generated by negative drift, it is possible to enrich for normally motile yet nonchemotactic mutants. The factor achieved in a single pass (40), while not impressive, is nevertheless respectable. In the past, selections of this kind have only been possible for nonchemotactic cells that swim smoothly. These cells tend to sediment, cell body faster than flagellar bundle, and thus tilt front-end downward; they swim to the bottom of a column of liquid stabilized against convective stirring (cf. Aswad and Koshland, 1975). The problem is that wild-type cultures invariably contain a significant proportion of cells that fail to do chemotaxis because they have suffered temporary loss of flagella or some other physiological misfortune (Parkinson, 1987). It is not sufficient to look for cells that, for whatever reason, fail to do chemotaxis. Rather, it is essential that the cells selected be vigorously motile. This criterion is met in our procedure, because cells that are selected must swim from one chamber to the other. Because smooth-swimming cells can do this more readily than tumbly cells (Table 3), smooth-swimming cells are favored. However, they do not have a strong advantage over cells with wild-type motility.

One of the issues that stimulated the present work was whether *cheRcheB* cells, mutants defective in both methylation and demethylation, are chemotactic (cf. Segall et al., 1986; Stock et al., 1985). Capillary assays appear to show small responses at low concentrations of aspartate (Stock et al., 1985). In the layered-gradient assay, responses to aspartate are not observed in shallow exponential gradients, but they are detected near the boundary of a large step (Weis and Koshland, 1988). Our data (Table 5) argue that chemotactic responses of *cheRcheB* cells, if any, are small, generating drift velocities of order 1% of that of the wild type or less. The responses were negligible in gradients of aspartate or serine in the presence of a uniform concentration of serine or aspartate, respectively.

We thank Frank Dailey for preparation of strain HCB869, Win Hill for electronic design, Markus Meister for help with the mathematics, Don Rogers for fabrication of mechanical components, and Karen Fahrner, Ed Purcell, and Beat Stolz for comments on the manuscript.

This work was supported by the Rowland Institute for Science and by grant AI16478 from the National Institute of Allergy and Infectious Diseases.

Received for publication 30 April 1990 and in final form 20 June 1990.

REFERENCES

Adler, J. 1966. Chemotaxis in bacteria. *Science* (*Wash. DC*). 153:708–716.

Adler, J. 1969. Chemoreceptors in bacteria. *Science* (*Wash. DC*). 166:1588–1597.

Adler, J. 1973. A method for measuring chemotaxis and use of the

method to determine optimum conditions for chemotaxis in *Escherichia coli*. *J. Gen. Microbiol.* 74:77–91.

Armitage, J. P., D. P. Josey, and D. G. Smith. 1977. A simple quantitative method for measuring chemotaxis and motility in bacteria. *J. Gen. Microbiol.* 102:199–202.

Armstrong, J. B., and J. Adler. 1969. Location of genes for motility and chemotaxis on the *Escherichia coli* genetic map. *J. Bacteriol.* 97:156–171.

Armstrong, J. B., J. Adler, and M. M. Dahl. 1967. Nonchemotactic mutants of *Escherichia coli*. *J. Bacteriol.* 93:390–398.

Aswad, D., and D. E. Koshland, Jr. 1975. Isolation, characterization and complementation of *Salmonella typhimurium* chemotaxis mutants. *J. Mol. Biol.* 97:225–235.

Berg, H. C. 1971. How to track bacteria. *Rev. Sci. Instrum.* 42:868–871.

Berg, H. C. 1978. The tracking microscope. *Adv. Opt. Elec. Microsc.* 7:1–13.

Berg, H. C. 1983. Random Walks in Biology. Princeton University Press, Princeton. 142 pp.

Berg, H. C. 1988. A physicist looks at bacterial chemotaxis. *Cold Spring Harbor Symp. Quant. Biol.* 53:1–9.

Berg, H. C., and S. M. Block. 1984. A miniature flow cell designed for rapid exchange of media under high-power microscope objectives. *J. Gen. Microbiol.* 130:2915–2920.

Berg, H. C., and D. A. Brown. 1972. Chemotaxis in *Escherichia coli*. analysed by three-dimensional tracking. *Nature* (*Lond.*). 239:500–504.

Bevington, P. R. 1969. Data reduction and Error Analysis for the Physical Sciences. McGraw-Hill, New York. 64.

Block, S. M., and H. C. Berg. 1984. Successive incorporation of force-generating units in the bacterial rotary motor. *Nature* (*Lond.*). 309:470–472.

Block, S. M., J. E. Segall, and H. C. Berg. 1983. Adaptation kinetics in bacterial chemotaxis. *J. Bacteriol.* 154:312–323.

Born, M., and E. Wolf. 1980. Principles of Optics. 6th ed. Pergamon Press, Oxford. 655–656.

Bourret, R. B., J. F. Hess, K. A. Borkovich, A. A. Pakula, and M. I. Simon. 1989. Protein phosphorylation in chemotaxis and two-component regulatory systems of bacteria. *J. Biol. Chem.* 264:7085–7088.

Chang, Y.-Y., and J. E. Cronan, Jr. 1982. Mapping nonselectable genes of *Escherichia coli* by using transposon Tn*10*: location of a gene affecting pyruvate oxidase. *J. Bacteriol.* 151:1279–1289.

Clarke, S., and D. E. Koshland, Jr. 1979. Membrane receptors for aspartate and serine in bacterial chemotaxis. *J. Biol. Chem.* 254:9695–9702.

Dahlquist, F. W., P. Lovely, and D. E. Koshland, Jr. 1972. Quantitative analysis of bacterial migration in chemotaxis. *Nature New Biol.* 236:120–123.

Dahlquist, F. W., R. A. Elwell, and P. S. Lovely. 1976. Studies of bacterial chemotaxis in defined concentration gradients. A model for chemotaxis toward L-serine. *J. Supramol. Struct.* 4:329–342.

Khan, S., and H. C. Berg. 1983. Isotope and thermal effects in chemiosmotic coupling to the flagellar motor of Streptococcus. *Cell.* 32:913–919.

Lengeler, J. W., and A. P. Vogler. 1989. Molecular mechanisms of bacterial chemotaxis toward PTS-carbohydrates. *FEMS Microbiol. Rev.* 63:81–92.

Lowe, G., M. Meister, and H. C. Berg. 1987. Rapid rotation of flagellar bundles in swimming bacteria. *Nature* (*Lond.*). 325:637–640.

Macnab, R. M. 1987*a*. Flagella. *In Escherichia coli* and *Salmonella typhimurium*: Cellular and Molecular Biology. F. C. Neidhardt, J. L. Ingraham, K. Brooks Low, Boris Magasanik, and Moselio Schaechter, editors. American Society for Microbiology, Washington, DC. 1:70–83.

Macnab, R. M. 1987*b*. Motility and chemotaxis. *In Escherichia coli:* and *Salmonella typhimurium* : Cellular and Molecular Biology. F. C. Neidhardt, J. L. Ingraham, K. Brooks Low, Boris Magasanik, and Moselio Schaechter, editors. American Society for Microbiology, Washington, DC. 1:732–759.

Macnab, R. M., and D. J. DeRosier. 1988. Bacterial flagellar structure and function. *Can. J. Microbiol.* 34:442–451.

Nossal, R. 1972. Growth and movement of rings of chemotactic bacteria. *Exp. Cell. Res.* 75:138–142.

Nossal, R., and G. H. Weiss. 1973. Analysis of a densitometry assay for bacterial chemotaxis. *J. Theor. Biol.* 41:143–147.

Parkinson, J. S. 1987. Doing behavioral genetics with bacteria. *Genetics.* 116:499–500.

Schnitzer, M. J., S. M. Block, H. C. Berg, and E. M. Purcell. 1990. Strategies for chemotaxis. *Symp. Soc. Gen. Microbiol.* In press.

Segall, J. E., S. M. Block, and H. C. Berg. 1986. Temporal comparisons in bacterial chemotaxis. *Proc. Natl. Acad. Sci. USA.* 83:8987–8991.

Segel, L. A., and J. L. Jackson. 1973. Theoretical analysis of chemotactic movement in bacteria. *J. Mechanochem. Cell Motil.* 2:25–34.

Segel, L. A., I. Chet, and Y. Henis. 1977. A simple quantitative assay for bacterial motility. *J. Gen. Microbiol.* 98:329–337.

Sherris, D., and J. S. Parkinson. 1981. Posttranslational processing of methyl-accepting chemotaxis proteins in *Escherichia coli*. *Proc. Natl. Acad. Sci. USA.* 78:6051–6055.

Stewart, R. C., and F. W. Dahlquist. 1987. Molecular components of bacterial chemotaxis. *Chem. Rev.* 87:997–1025.

Stock, J., A. Borczuk, F. Chiou, and J. E. B. Burchenal. 1985. Compensatory mutations in receptor function: a reevaluation of the role of methylation in bacterial chemotaxis. *Proc. Natl. Acad. Sci. USA.* 82:8364–8368.

Stock, J. B., A. M. Stock, and J. M. Mottonen. 1990. Signal transduction in bacteria. *Nature* (*Lond.*). 344:395–400.

Weis, R. M., and D. E. Koshland, Jr. 1988. Reversible receptor methylation is essential for normal chemotaxis of *Escherichia coli* in gradients of aspartic acid. *Proc. Natl. Acad. Sci. USA.* 85:83–87.

Wolfe, A. J., and H. C. Berg. 1989. Migration of bacteria in semi-solid agar. *Proc. Natl. Acad. Sci. USA.* 86:6973–6977.

Wolfe, A. J., M. P. Conley, T. J. Kramer, and H. C. Berg. 1987. Reconstitution of signaling in bacterial chemotaxis. *J. Bacteriol.* 169:1878–1885.

Wolfe, A. J., M. P. Conley, and H. C. Berg. 1988. Acetyladenylate plays a role in controlling the direction of flagellar rotation. *Proc. Natl. Acad. Sci. USA.* 85:6711–6715.